Inorganic Chemistry

pubs.acs.org/IC

Article

Tuning the Properties of Rigidified Acyclic DEDPA^{2-} Derivatives for Application in PET Using Copper-64

Daniel Torralba-Maldonado, Axia Marlin, Fátima Lucio-Martínez, Antía Freire-García, Jennifer Whetter, Isabel Brandariz, Emilia Iglesias, Paulo Pérez-Lourido, Rosa M. Ortuño, Eszter Boros,* Ona Illa,* David Esteban-Gómez, and Carlos Platas-Iglesias*

Cite This: *Inorg. Chem.* 2024, 63, 22297−22307

ABSTRACT: We present a detailed investigation of the coordination chemistry toward [^{nat}Cu/^{64}Cu]copper of a series of H_2DEDPA derivatives (H_2DEDPA = 6,6′-((ethane-1,2-diylbis(azanediyl))bis(methylene))-dipicolinic acid) containing cyclohexyl (H_2CHXDEDPA), cyclopentyl (H_2CpDEDPA) or cyclobutyl (H_2CBuDEDPA) spacers. Furthermore, we also developed a strategy that allowed the synthesis of a H_2CBuDEDPA analogue containing an additional NHBoc group at the cyclobutyl ring, which can be used for conjugation to targeting units. The X-ray structures of the Cu(II) complexes evidence distorted octahedral coordination around the metal ion in all cases. Cyclic voltammetry experiments (0.15 M NaCl) evidence quasi-reversible reduction waves associated with the reduction of Cu(II) to Cu(I). The complexes show a high thermodynamic stability, with log K_{CuL} values of 25.11(1), 22.18(1) and 20.19(1) for the complexes of CHXDEDPA^{2-}, CpDEDPA^{2-} and CBuDEDPA^{2-}, respectively (25 °C, 1 M NaCl). Dissociation kinetics experiments reveal that both the spontaneous- and proton-assisted pathways operate at physiological pH. Quantitative labeling with $^{64}CuCl_2$ was observed at 0.1 nmol for CHXDEDPA^{2-} and CpDEDPA^{2-}, 0.025 nmol for CBuDEDPA^{2-} and 1 nmol for CBuDEDPA-NHBoc^{2-}, with no significant differences observed at 15, 30, and 60 min. The radio-complexes are stable in PBS over a period of 24 h.

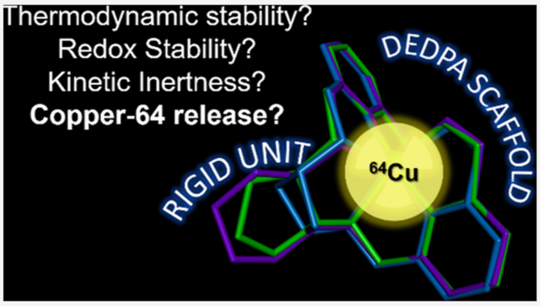

■ INTRODUCTION

Among the radionuclides with interesting properties for positron emission tomography (PET) is copper-64, which decays with a half-life of $t_{1/2}$ = 12.7 h through electron capture (43.9%) and β^- (38.5%) and β^+ (17.6%) decays, and can be produced both using reactors and cyclotrons.[1,2] The development of ^{64}Cu-based radiopharmaceuticals requires the preparation of bifunctional chelators, which incorporate a metal ion binding site and a coupling function separated by a spacer. The coupling function is used to link the chelator to a targeting unit, which is responsible for taking the probe to the desired target in vivo.

In 2020, the Food and Drug Administration approved the first ^{64}Cu-based radiopharmaceutical for clinical use, [^{64}Cu]Cu-DOTATATE, which is based on a DOTA chelating unit and was shown to provide similar results to [^{68}Ga]Ga-DOTATATE.[3] Despite their widespread use, it is well-known that DOTA derivatives are not ideal chelators for Cu^{2+}, with NOTA performing significantly better (Chart 1).[4−7] The number of ^{64}Cu-based radiopharmaceuticals entering clinical trials is growing rapidly,[8] with current candidates being most commonly based on DOTA,[9] NOTA,[10] cyclam cross-bridge derivatives such as CB-TE1A1P[11] and sarcophagine.[12,13] However, the seek for new efficient chelators remains an active area of research.[14−23] In particular, the biodistribution of the radioconjugate may be significantly affected by the nature of the bifunctional chelator if peptides are used as targeting units.[24] Thus, it is important to expand the library of currently available chelators suitable for ^{64}Cu-based radiopharmaceuticals.

The acyclic chelator H_2DEDPA and the rigidified derivative H_2CHXDEDPA[25] were highlighted as very promising chelators for the development of ^{68}Ga-based radiopharmaceuticals (Chart 1).[26,27] Early studies performed on H_2DEDPA derivatives evidenced poor stability in serum of the radiolabeled [^{64}Cu(DEDPA)] complex,[28] while the [^{64}Cu(CHXDEDPA)] complex is 98% stable after 24 h in human serum at 37 °C.[29] This striking different behavior highlights the beneficial effect that introducing a rigid cyclohexyl group has in the stability of the ^{64}Cu-labeled complexes. A number of structural modifications were introduced to the H_2DEDPA

Received: September 23, 2024
Revised: October 22, 2024
Accepted: October 28, 2024
Published: November 7, 2024

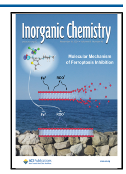

https://doi.org/10.1021/acs.inorgchem.4c04050
Inorg. Chem. 2024, 63, 22297−22307

Chart 1. Structures of Ligands Discussed in the Present Work

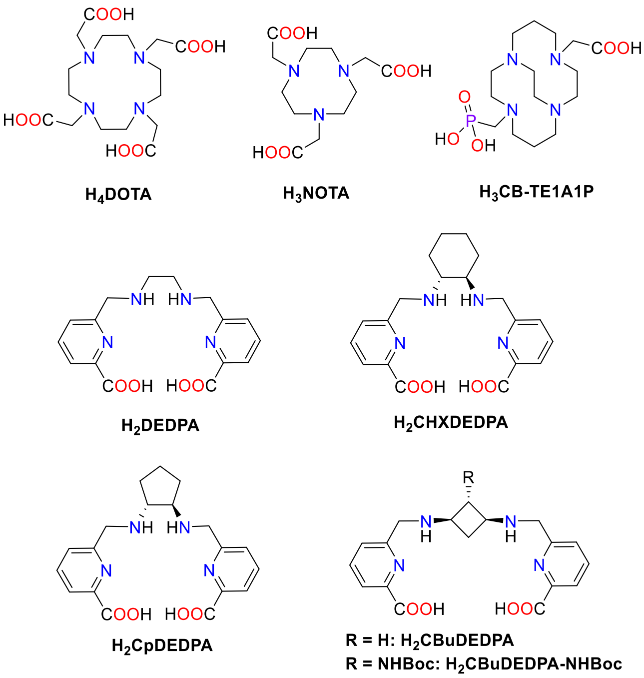

scaffold to obtain bifunctional derivatives[26] or to introduce redox-active[29] or fluorescent[30] units. *N*-alkylation[31] and functionalization of position 4 of the pyridyl rings[30] of H_2DEDPA were found to be detrimental for the radiolabeling efficiency and/or stability of the radiolabeled ^{68}Ga-labeled complexes, with C-functionalization being the most promising strategy.[26] The situation appears to be somewhat different for ^{64}Cu-derivatives, with some studies demonstrating an increased stability of *N*-alkylated derivatives.[32,33]

Considering the very promising properties of H_2DEDPA compounds for the development of ^{64}Cu-based radiopharmaceuticals, we envisaged to expand the family of rigid derivatives and analyze their potential for ^{64}Cu-based radiopharmaceutical development. Furthermore, we also aimed at developing the synthetic methodology required to prepare *C*-functionalized derivatives of H_2DEDPA, gaining access to bifunctional ligands. Thus, we have modified the ethylene bridge of H_2DEDPA by introducing rigid units to give the corresponding cyclopentyl ($H_2CpDEDPA$) and cyclobutyl ($H_2CBuDEDPA$) compounds. The coordination chemistry properties of these chelators were then compared with those of the cyclohexyl analogue $H_2CHXDEDPA$ (Chart 1). The $H_2CHXDEDPA$ ligand was reported in 2008 and studied for Ni(II), Zn(II), Cd(II) and Pb(II) complexation.[25,34] The $H_2CBuDEDPA$ ligand was reported recently and used for Fe(III) complexation,[35] while $H_2CpDEDPA$ is reported here for the first time. 1,2-Cyclobutanediamine-based ligands had been described before for the complexation of Gd(III) and Mn(II),[36,37] demonstrating that the rigidity of the 4-membered carbocycle used as spacer enhanced the kinetic inertness of the resulting complexes.

■ RESULTS AND DISCUSSION

Syntheses. The synthesis of the $H_2CpDEDPA$ ligand was achieved by reaction of commercially available *trans*-1,2-cyclopentanediamine and methyl 6-formylpyridine-2-carboxylate,[38] followed by reduction of the intermediate Schiff-base with $NaBH_4$. Hydrolysis of the methyl ester groups in 6 M HCl and purification using reverse-phase chromatography afforded the ligand in 48% yield.

The synthesis of the protected bifunctional ligand $H_2CBuDEDPA$-NHBoc was achieved following the strategy presented in Scheme 1 (see Supporting Information for details). The synthesis started from previously reported trifunctionalized cyclobutane derivative **1**,[39] which affords a protected alcohol and a carboxyl group as precursors of the *cis*-1,3-diamino system. To epimerize the α-position to the carboxyl group, compound **1** was converted temporarily into a mixed acid anhydride, which was subsequently hydrolyzed to give **2** as the major product in a 5:1 mixture together with starting material **1** (76% yield over the two steps). This mixture was subjected to a Curtius rearrangement using diphenylphosphoryl azide under reflux and the resulting isocyanate was reacted with benzyl alcohol to yield dicarbamate **3** in 81% yield after purification. Deprotection of the hydroxyl group in **3** was carried out using neat TFA. This reaction also implied the acidolysis of the *tert*-butylcarbamate. The resulting amine was reprotected using di-*tert*-butyl dicarbonate, **4** being obtained in 87% yield over the two steps. After that, a Mitsunobu reaction was carried out in order to install an azide in place of the hydroxyl group with

Scheme 1. Synthesis of the Bifunctional precursor $H_2CBuDEDPA$-NHBoc

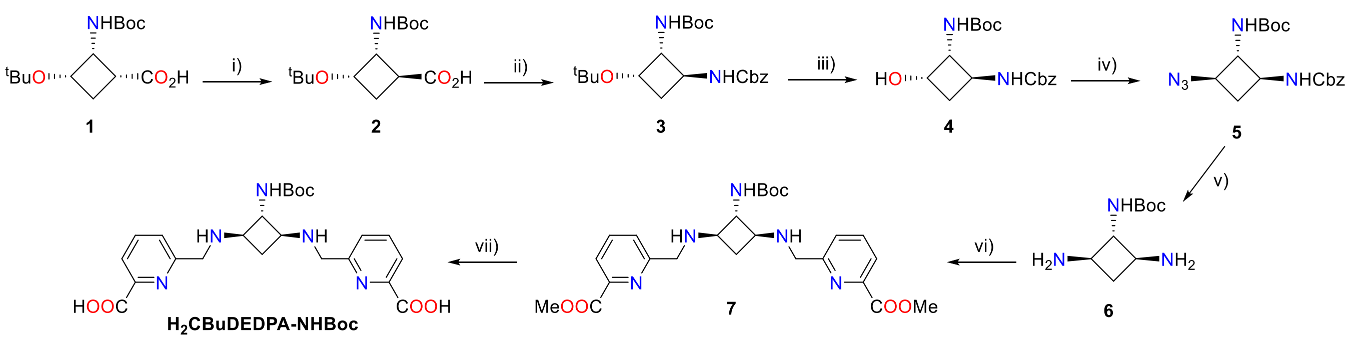

[a]Reagents and conditions: (i) (a) Boc_2O, pyridine, NH_4HCO_3, dioxane, 0 °C to rt, 4 h; (b) 6.25 M NaOH, MeOH, reflux, 18 h, 76%; (ii) (a) DPPA, Et_3N, toluene, reflux, 2 h; (b) BnOH, 80 °C, 6 h, 81%; (iii) (a) TFA, 0 °C to rt, 3 h; (b) Boc_2O, Et_3N, THF, 0 °C to rt, 4 h, 87%; (iv) DPPA, PPh_3, DIAD, THF, 0 °C to rt, 3 h, 79%; (v) H_2, Pd/C, MeOH, rt, 16 h, Quantitative; (vi) (a) methyl 6-formylpicolinate, MeOH, 40 °C, 2.5 h; (b) $NaBH_3CN$ 0 °C to rt, 4 h, 50%.; (vii) LiOH, H_2O:THF, rt, 3 h, 53%

https://doi.org/10.1021/acs.inorgchem.4c04050
Inorg. Chem. 2024, 63, 22297−22307

inversion of configuration, which afforded **5** in 79% yield. Subsequently, Pd-catalyzed hydrogenolysis of the benzyl carbamate and reduction of the azide group led to triamine **6** in quantitative yield. Compound **6** was submitted to double reductive amination with methyl 6-formylpicolinate,[38] rendering orthogonally protected precursor **7** in 50% yield. The saponification of the methyl ester groups with LiOH afforded the desired bifunctional *all-trans*-triamine ligand H_2CBuDEDPA-NHBoc, which contains a spacer bearing a protected amino group suitable for conjugation. The ligand was obtained in a 7-step sequence in 11% overall yield.

The Cu(II) complexes of $CHXDEDPA^{2-}$, $CpDEDPA^{2-}$ and $CBuDEDPA^{2-}$ were synthesized by reaction of the corresponding ligand with $Cu(OTf)_2$ in aqueous solution at pH ~7 and isolated in ~50% yields after purification through reverse-phase chromatography using a C18AQ column (see Supporting Information for details). The UV−vis absorption spectra of the three complexes are very similar (Figure S27, Supporting Information), showing d−d absorption bands at 720 ([Cu(CHXDEDPA)]), 732 ([Cu(CpDEDPA)]) and 728 nm ([Cu(CBuDEDPA)]) ($\varepsilon \sim 75$ M^{-1} cm^{-1}). These absorption data are very similar to those reported for $[Cu(OCTAPA)]^{2-}$ and [Cu(DEDPA)], which have distorted N_4O_2 octahedral coordination.[40] This indicates that the nature of the spacer has little impact on the structures of these complexes in solution.

X-ray Structures. Single crystals were obtained by slow diffusion of acetone into aqueous solutions of the Cu(II) complexes. Crystals contain the charge neutral complexes and solvent molecules (water and/or acetone). The bond distances of the Cu(II) coordination sphere are listed in Table 1, while views of the structures of the complexes are shown in Figure 1 (see Table S3 for bond angles). The metal ions are coordinated to the six donor atoms of the ligand, which wraps around the metal ion to offer a distorted octahedral coordination environment. However, the bond angles of the metal coordination sphere evidence a strong distortion of the octahedral coordination, with *trans* angles in the range of ~149−169°. Furthermore, the bond distances of the metal coordination environment involving the same type of donor atom differ significantly, which is characteristic of six-coordinate Cu(II) complexes with Jahn−Teller distortion.[41,42] This effect is particularly pronounced for the Cu(1)−O(1) and Cu(1)−O(3) distances, which differ by 0.181, 0.224, and 0.179 Å for [Cu(CHXDEDPA)], [Cu(CpDEDPA)] and [Cu(CBuDEDPA)], respectively. Similar distortions of the metal coordination sphere were observed previously for [Cu(DEDPA)] and *N*-alkylated derivatives of H_2CHXDEDPA.[28,29]

Table 1. Bond Distances of the Cu(II) Coordination Environments Determined by Single-Crystal X-ray Measurements and Shape Measures for Octahedral and Trigonal Prismatic Coordination[a]

	$CHXDEDPA^{2-}$	$CpDEDPA^{2-}$	$CBuDEDPA^{2-}$
Cu(1)−N(1)	1.9283(17)	1.916(2)	1.944(2)
Cu(1)−N(2)	2.1429(19)	2.122(2)	2.156(2)
Cu(1)−N(3)	2.2651(19)	2.303(3)	2.258(2)
Cu(1)−N(4)	1.9748(17)	1.962(2)	1.993(2)
Cu(1)−O(1)	2.0961(15)	2.079(2)	2.1102(18)
Cu(1)−O(3)	2.2771(15)	2.294(2)	2.2887(18)
S(OC-6)[a]	4.786	4.629	3.541
S(TPR-6)[a]	6.243	6.375	9.581

[a]Shape measures for octahedral, S(OC-6), and trigonal prismatic S(TPR-6), coordination.

Shape measurements were conducted to assess the degree of distortion of the metal coordination environment.[43−45] The [Cu(CHXDEDPA)] and [Cu(CpDEDPA)] complexes are characterized by similar Shape measures for an octahedral coordination [S(OC-6), Table 1], while a trigonal prismatic coordination affords higher Shape measures [S(TPR-6), Table 1]. This indicates that the coordination environment is best described as octahedral, though rather distorted (an ideal octahedral coordination is characterized by S(OC-6) = 0). Shape measures indicate that the octahedral coordination in [Cu(CBuDEDPA)] is less distorted than in [Cu(CHXDEDPA)] and [Cu(CpDEDPA)]. The Shape measures obtained for this series of structurally related compounds differ significantly from those characterizing the minimal distortion pathway between an octahedron and a trigonal prism (Figure S23, Supporting Information),[46] which reflects the constraints on the metal coordination environment imposed by these rigid ligands.

Cyclic Voltammetry. Cyclic voltammetry experiments were carried out to assess the stability of the Cu(II) complexes toward reduction. A recent study demonstrated that the redox potential of Cu(II) complexes must be shifted out of the window of bioreducing agents like ascorbate, as even very inert Cu(II) complexes can dissociate quickly upon reduction to Cu(I).[47] The threshold of bioreducing agents was estimated to be −0.4 V versus NHE.[48]

The cyclic voltammograms (50 mV/s) recorded from aqueous solutions of the complexes in 0.15 M NaCl (vs Ag/AgCl) display quasi-reversible features with half-wave potentials $E_{1/2}$ = −695 mV (ΔE_p = 149 mV), $E_{1/2}$ = −618 mV (ΔE_p = 73 mV) and $E_{1/2}$ = −565 mV (ΔE_p = 120 mV) for [Cu(CHXDEDPA)], [Cu(CpDEDPA)] and [Cu(CBuDEDPA)], respectively (Figure 2). For all three complexes ΔE_p increases upon increasing the scan rate, in line with electrochemically quasi-reversible processes. The peak current varies linearly with the square-root of the scan rate, which suggests that the electrochemical processes are diffusion-controlled (Figures S24−S26, Supporting Information).[49] The cyclic voltammograms show a second irreversible oxidation wave that is more prominent at low scan rates, most likely arising from the structural reorganization of the reduced Cu(I) species. This irreversible oxidation wave is particularly prominent at −160 mV for [Cu(CHXDEDPA)] (Figure 2). Of note, the cyclic voltammogram reported for [Cu(DEDPA)] shows an irreversible reduction peak at −1.12 V (vs Ag/AgCl),[28] as well as an oxidative stripping peak of Cu(0) to Cu(II) around 0.0 V[50] that indicates dissociation of the Cu(I) complex within the time scale of the experiment. This is indicative of an increased stability upon reduction of the rigid derivatives described here with respect to the parent [Cu(DEDPA)] complex.

The reduction potential of [Cu(CHXDEDPA)] is clearly out of the threshold of common bioreductants ($E_{1/2}$ = −695 mV versus Ag/AgCl corresponds to −475 mV versus NHE).[51] The reduction potentials determined by cyclic voltammetry for [Cu(CpDEDPA)] and [Cu(CBuDEDPA)] are right on the edge of this threshold.

The $E_{1/2}$ values obtained for this series of complexes indicate that the ability to stabilize Cu(I) increases following the trend $CBuDEDPA^{2-}$ > $CpDEDPA^{2-}$ > $CHXDEDPA^{2-}$. This can be

https://doi.org/10.1021/acs.inorgchem.4c04050
Inorg. Chem. 2024, 63, 22297−22307

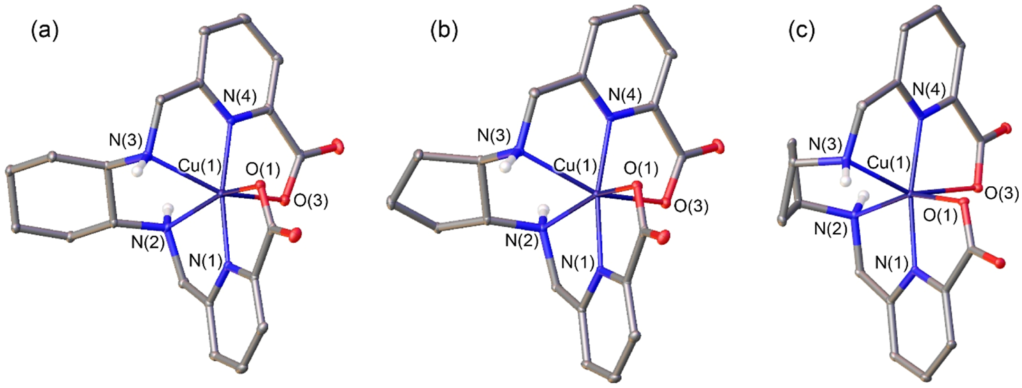

Figure 1. X-ray structures of: (a) $[Cu(CHXDEDPA)]\cdot(CH_3)_2CO\cdot H_2O$, (b) $[Cu(CpDEDPA)]\cdot 4H_2O$ and (c) [Cu(CBuDEDPA)] with ellipsoids plotted at the 30% probability level. Solvent molecules and H atoms bonded to C atoms are omitted for simplicity.

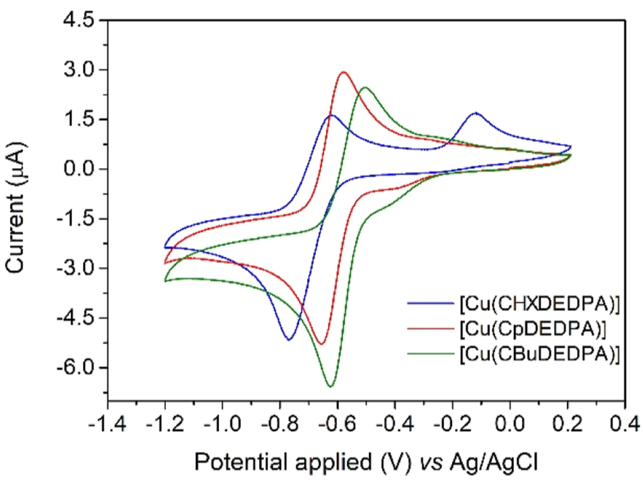

Figure 2. Cyclic voltammograms recorded from aqueous solutions of the Cu(II) complexes (0.15 M NaCl, scan rate 50 mV/s). Conditions: [Cu(CHXDEDPA)], 1.4 mM, pH 6.6; [Cu(CpDEDPA)], 1.3 mM, pH 6.9; [Cu(CBuDEDPA)], 1.3 mM, pH 5.0.

correlated with the ability of the ligand to provide an octahedral coordination with Jahn–Teller distortion. The Jahn–Teller distortion provides an additional stability to six-coordinate Cu(II) complexes,[52] a contribution that is evidenced in the Irving-Williams order.[53] A more negative $E_{1/2}$ value is therefore expected for complexes having a larger shape measure for octahedral distortion (S(OC-6), Table 1), due to a limited stability enhancement due to the Jahn–Teller effect.

Thermodynamic Stability. The protonation constants of the $DEDPA^{2-}$ derivatives investigated here were determined using potentiometric titrations. The Cu(II) complexes of these ligands dissociate at rather low pH values, which prevented complex stability constant determination using direct methods and an ionic strength of I = 0.15 M NaCl. Thus, we determined the protonation constants of $CHXDEDPA^{2-}$ using I = 1.0 M NaCl as the ionic strength. The protonation constants determined here using I = 1.0 M NaCl compare well with those reported in 0.15 M NaCl[27] and 0.1 M $(Me_4N)(NO_3)$,[25] which indicates that the different nature and concentration of the background electrolyte does not have a significant impact on the protonation constants (Table 2).

The first and second protonation constants (log K_1^H and log K_2^H) correspond to the protonation of the amine N atoms of the ligand. The value of log K_1^H increases slightly on replacing the central ethyl group of $DEDPA^{2-}$ by a cyclohexyl ring. A similar effect was observed previously for the first protonation constant of $EDTA^{4-}$ and the cyclohexyl derivative $CDTA^{4-}$.[54] This can be attributed, at least in part, to the electron-donating effect of the ring.[55] The value of log K_1^H decreases following the order $CHXDEDPA^{2-}$ > $CpDEDPA^{2-}$ > $CBuDEDPA^{2-}$, likely reflecting a decreased cooperation between the amine N atoms during the first protonation process.[56] The value of log K_2^H determined for $CBuDEDPA^{2-}$ is the highest among this series of closely related derivatives, which likely reflects a decreased electrostatic repulsion in the deprotonated form due to the large distance between the amine N atoms, which are placed at positions 1 and 3 of the cyclobutyl unit.

Table 2. Ligand Protonation Constants and Stability Constants of the Cu(II) Complexes Determined Using Potentiometric and Spectrophotometric Titrations (1 M NaCl, 25 °C)

	$CHXDEDPA^{2-}$	$CpDEDPA^{2-}$	$CBuDEDPA^{2-}$	$DEDPA^{2-c}$
I	1 M NaCl	1 M NaCl	1 M NaCl	1 M NaCl
log K_1^H	9.41(1)/9.23[a]/9.13[b]	9.05(1)	8.95(1)	9.00[c]/8.69[b]
log K_2^H	6.45(1)/6.47[a]/6.44[b]	6.51(2)	6.87(1)	6.30[c]/6.18[b]
log K_3^H	3.35(2)/2.99[a]/3.25[b]	3.28(3)	3.32(2)	3.06[c]/3.08[b]
log K_4^H	2.48(2)/2.40[a]/2.40[b]	2.51(4)	2.52(3)	2.59[c]/2.33[b]
Σ log K_i^H (i = 1–4)	21.69/21.09[a]/21.22[b]	22.18	20.19	20.95[c]
log K_{CuL}	25.11(1)	22.18(1)	20.19(1)	19.16[d]
pCu[e]	24.0	21.4	19.5	18.5

[a]Data in 0.15 M NaCl from ref 27. [b]Data in 0.1 M $(Me_4N)(NO_3)$ from ref 25. [c]Data in 0.15 M NaCl from ref 26. [d]Data in 0.15 M NaCl from ref 28. [e]Defined as−log $[Cu(II)]_{free}$, for $[L]_{tot}$ = 10 μM and $[Cu(II)]_{tot}$ = 1 μM.

https://doi.org/10.1021/acs.inorgchem.4c04050
Inorg. Chem. 2024, 63, 22297−22307

The stability constants of the Cu(II) complexes were determined using spectrophotometric titrations, as complex dissociation occurs in a pH range that is not appropriate for direct potentiometric titrations (<2.0, see Figures S28–S30, Supporting Information). The absorption spectra of the complexes display the characteristic absorption due to the picolinate chromophore at 270 nm. The intensity of this band decreases upon lowering the pH due to complex dissociation, eventually yielding the spectrum of the LH_4^{2+} species. To aid data analysis, the absorption spectrum of LH_4^{2+} was obtained independently and provided to the fitting program.

The fits of the spectrophotometric data (Figure 3, see also Figures S31–S32, Supporting Information) afford the stability

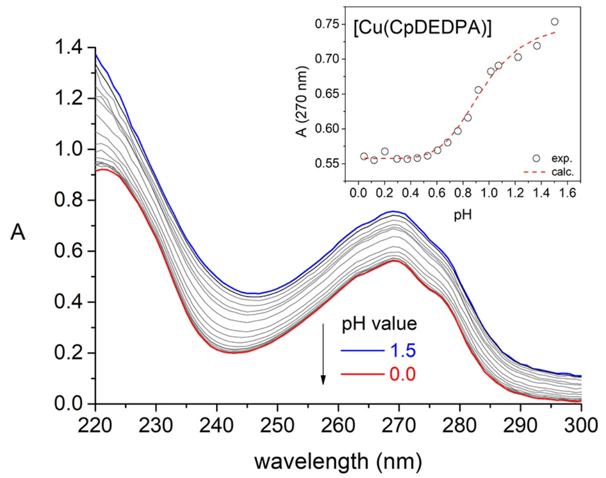

Figure 3. Spectrophotometric titration of [Cu(CpDEDPA)] (6.36 × 10^{-5}, I = 1 M NaCl) with pH. The inset shows the experimental absorbance values at 270 nm and the dashed line the fit of the data for stability constant determination.

constants shown in Table 2. The complex with CHXDEDPA^{2-} displays the highest thermodynamic stability constant among this series of complexes, with a remarkably high log K_{CuL} = 25.11. This represents an increase in complex stability of 6 orders of magnitude compared with DEDPA^{2-}. The stability constants of the Cu(II) complexes with these ligands follow the trend CHXDEDPA^{2-} > CpDEDPA^{2-} > CBuDEDPA^{2-}, the latter being still 1 order of magnitude higher than that reported for DEDPA^{2-}.[28] Thus, modification of the ligand scaffold by introducing a rigid spacer has a beneficial impact in terms of complex stability, an effect that is particularly pronounced for the cyclohexyl derivative CHXDEDPA^{2-}.

The stability of metal complexes for medical applications at physiological pH is generally assessed by their pM (pCu) values, which are often defined as−log $[Cu(II)]_{free}$ for a total metal concentration of 1 μM and a total ligand concentration of 10 μM.[57] The pCu values calculated under these conditions follow closely the trend observed for log K_{CuL} (Table 2). This is not surprising, given that DEDPA^{2-} and the three derivatives described here display similar basicities, as indicated by the sum of log K_i^H values determined for each ligand (Table 2).

The stability constants and pCu values determined here are comparable to those of complexes with ligands commonly used as ^{64}Cu chelators such as DOTA^{4-} (pCu = 17.6, 0.1 M KCl),[58] NOTA^{3-} (pCu = 18.4, 1.0 M $Na(ClO_4)$)[59,60] or bispa^{-} (pCu = 19.3, 0.1 M KNO_3).[61] Cross-bridge cyclam derivatives display very high stability constants (log K_{CuL} = 27.1 for CB-cyclam), though radiolabeling often requires high temperatures.[62]

Dissociation Kinetics. The kinetic inertness of the radiocomplexes is a key property for any radiopharmaceutical candidate. In the particular case of PET agents, the release of the radioisotope decreases the uptake of the probe in the target tissue and increases background noise. Often the inertness of the complex is tested in vitro by studying the acid-catalyzed dissociation under harsh acidic conditions, using acid concentrations of 1.0–6.0 M.[15,63–65] However, these conditions are far away from those found in vivo. We recently proposed an alternative method to assess dissociation kinetics of Cu(II) complexes in a pH range relatively close to physiological conditions.[47] In this approach, the dissociation reaction is triggered by the presence of ascorbate (AA) using neocuproine (NC) as a scavenger. Ascorbate reduces any free Cu(II) present in the solution to Cu(I), which forms a very stable complex with NC with a characteristic absorption band at 450 nm.[66] The [Cu(CHXDEDPA)] complex does not dissociate in the presence of ascorbate at pH 6.7 over the course of 3 h (Figure S33, Supporting Information). Thus, we investigated the dissociation of the representative [Cu(CBuDEDPA)] complex in the pH range of 5.4–7.5 to gain information on the pathways that can potentially lead to complex dissociation under physiological conditions. These experiments were conducted using phosphate buffer and a large excess of both NC and ascorbate to ensure pseudo-first-order conditions (see details in Figure 4 and 5).

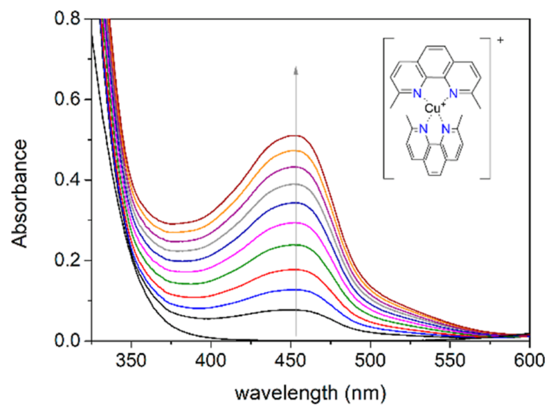

Figure 4. Spectral variations observed for a solution of [Cu(CBuDEDPA)] = 91 μM, [NC] = 0.24 mM, [AA] = 0.27 mM, [buffer] = 0.18 M. pH 6.7. Spectra were recorded every 6 min.

The observed dissociation rate constants k_{obs} do not vary with ascorbate concentration within experimental error (Table S4 and Figures S34–S35, Supporting Information). However, they increase with proton concentration, showing a saturation profile that indicates the formation of a protonated complex at the beginning of the reaction (Figure S36 and Table S5, Supporting Information). Thus, the observed first-order rate constants were fitted to eq 1

$$k_{obs} = \frac{k_0 + k_1 K_1^H[H^+]}{1 + K_1^H[H^+]} \quad (1)$$

Here, k_0 represents the rate constant for the spontaneous dissociation, while k_1 is the rate constant characterizing the proton-assisted dissociation and K_1^H is the protonation constant. The least-squares fit of the data affords k_0 = (8.2 ±

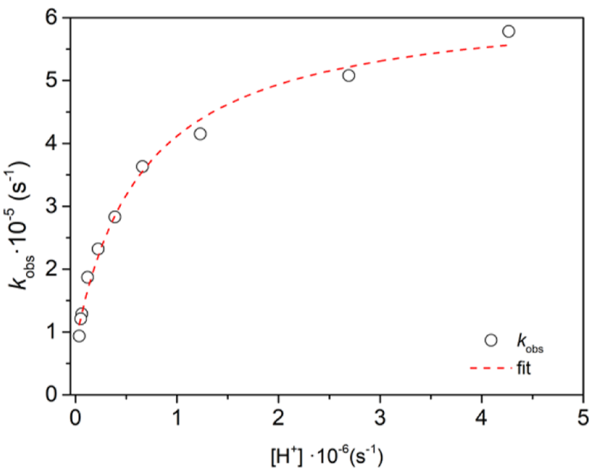

Figure 5. Dependence of the observed dissociation rate constants with proton concentration. Conditions: Spectral variations observed for a solution of [Cu(CBuDEDPA)] = 91 μM, [NC] = 0.24 mM, [AA] = 5.4 mM, [buffer] = 0.122 M.

1.3) $\times 10^{-6}$ s^{-1}, $k_1 = (6.3 \pm 0.2) \times 10^{-6}$ s^{-1} and $K_1^{H} = (1.5 \pm 0.2) \times 10^{6}$ M^{-1}. This kinetic data provide some unexpected results. First, this protonation constant corresponds to a pK_a of 6.2 that cannot be associated with any protonation constant of the octahedral complex. This pK_a value is actually only compatible with the protonation of an uncoordinated amino group. Thus, the kinetic data suggest that the proton-assisted dissociation pathway involves a kinetically active species in which amine N atoms are not directly coordinated to the metal. Second, the spontaneous dissociation pathway provides a significant contribution to the overall dissociation of the complex in the investigated pH range. However, at pH 7.4 the product $k_1K_1^{H}$[H$^+$] is 1 order of magnitude smaller than k_0, and thus the spontaneous dissociation mechanism becomes dominant. In spite of this, the [Cu(CBuDEDPA)] complex is remarkably inert considering its acyclic nature, with a half-life at pH 7.4 of 23.7 h. Kinetic experiments performed in concentrated acid solutions are unlikely to provide information on the spontaneous pathway, which is likely negligible under those conditions.

^{64}Cu Radiolabeling Experiments. The ability of the DEDPA-based ligands to coordinate ^{64}Cu was determined by probing radiochelation at 25 °C in 0.5 M ammonium acetate buffer pH 5.5 with 50−90 μCi of ^{64}CuCl$_2$. Labeling efficiency was quantified via radio-TLC (Figure S37, Supporting Information). The Apparent Molar Activity (AMA) for each chelator at 15, 30, and 60 min was determined and is summarized in Table S6 (Supporting Information). Figure 6 shows the results of concentration dependent radiolabeling for all tested ligands. CBuDEDPA^{2-} produced quantitative radiolabeling at an AMA of 4.939 Ci·μmol^{-1} (Figure 6c). The CHXDEDPA^{2-} and CpDEDPA^{2-} chelators produced AMA values of 0.631 Ci·μmol^{-1} and 0.565 Ci·μmol^{-1} respectively (Figure 6a and 6b). Complexation experiments of CBuDEDPA-NHBoc^{2-} (Figure 6d) with ^{64}Cu produced a specific molar activity of 3.563 Ci μmol^{-1}, thus remaining at the same order of magnitude as the parent ligand structure. Quantitative labeling was observed at 0.1 nmol for CHXDEDPA^{2-} and CpDEDPA^{2-}, 0.025 nmol for CBuDEDPA^{2-} and 1 nmol for CBuDEDPA-NHBoc^{2-} with no significant difference between 15, 30, and 60 min. The inertness of the formulated ^{64}Cu complexes was evaluated in PBS, evidencing no significant decomplexation of the radiocomplexes over 24 h (Table S7, Supporting Information). In addition, the ^{64}Cu complex integrity was investigated using 100× excess of diethylenetriaminepentaacetic acid (DTPA). Transchelation was monitored by TLC over the course of 24 h

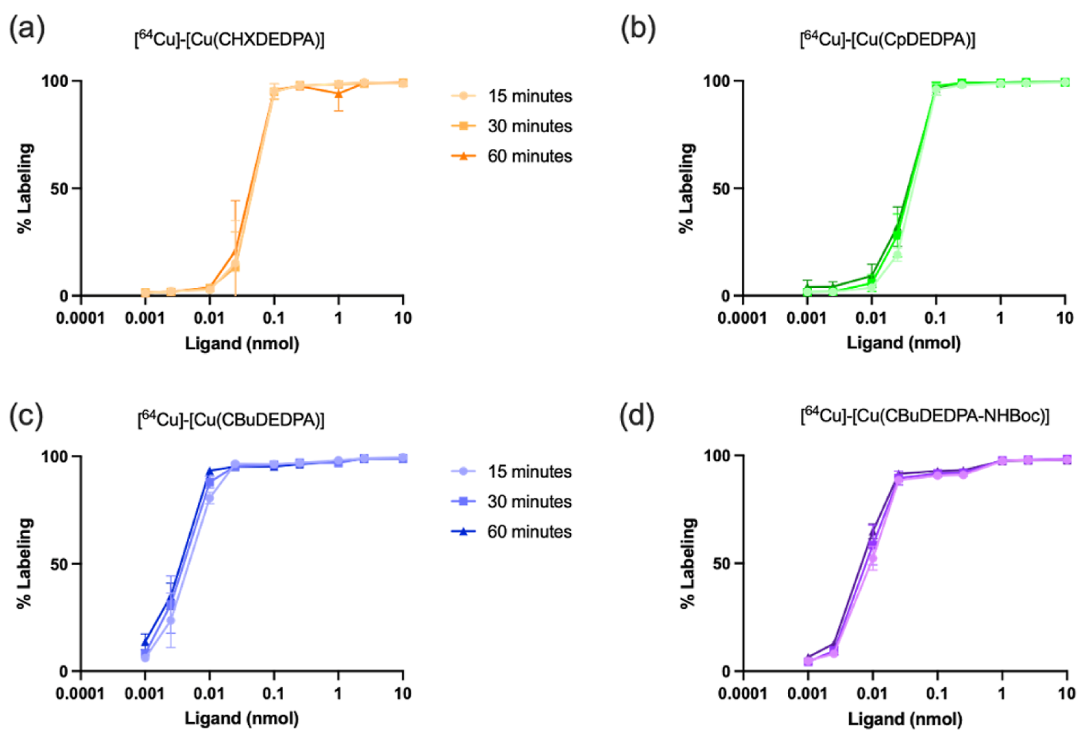

Figure 6. AMA determination curves for all chelator tested, with reaction yields analyzed at 3 time points, with $n = 3$ per data point. Activity per sample was 50−90 μCi with a total volume of 116 μL in 0.5 M ammonium acetate buffer pH 5.5.

https://doi.org/10.1021/acs.inorgchem.4c04050
Inorg. Chem. 2024, 63, 22297−22307

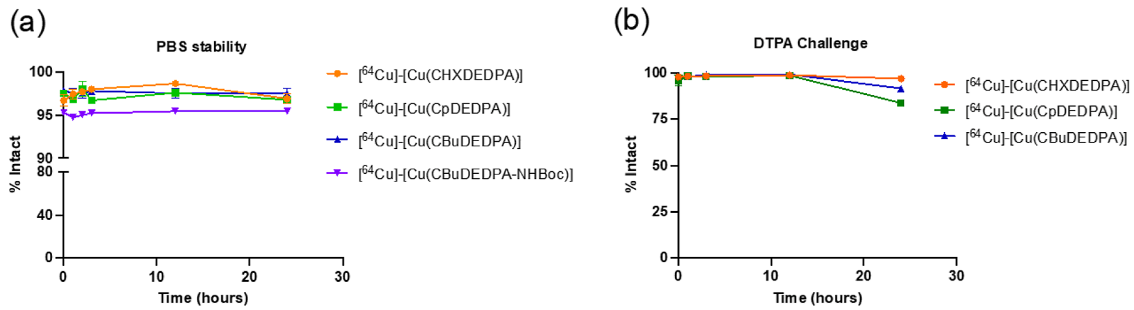

Figure 7. PBS stability (a) and DTPA challenge (b) of the ^{64}Cu-complexes. Ligand = 1 nmol, DTPA = 100 nmol, n = 3.

(Figure 7, see also Table S8, Supporting Information). The inertness of CpDEDPA^{2-} is lower than that of CHXDEDPA^{2-} and CBuDEDPA^{2-} with 83.7 ± 1.5% intact at 24 h versus 96.9 ± 0.6% and 91.6 ± 1.8%, respectively. However, quantitative transchelation was observed for CBuDEDPA-NHBoc^{2-} at the 10 min time point, indicating that the presence of a bulky substituent at position 2 of the cyclobutyl ring has a negative impact in the stability of the radio-complex.

■ CONCLUSIONS

We have investigated the coordination chemistry of a series of DEDPA^{2-} derivatives with [^{nat}Cu/^{64}Cu]copper by changing the nature of the central spacer. The analysis of the X-ray structures evidences that the nature of the spacer has a relatively minor impact in the metal coordination environment, although this subtle differences have some effect on the ability of the chelator to stabilize Cu(I). All three chelators containing rigid spacers form Cu(II) complexes with higher thermodynamic stability than the parent DEDPA^{2-} ligand, with stability following the sequence CHXDEDPA^{2-} > CpDEDPA^{2-}> CBuDEDPA^{2-}. The dissociation kinetics of the [Cu(CBuDEDPA)] complex were investigated close to physiological pH. This methodology allowed to identify both the spontaneous and proton-assisted pathways as responsible for the dissociation of the complex close to neutral pH. In contrast, dissociation experiments using high acid concentrations are unlikely to afford information on the spontaneous dissociation mechanism. The three chelators can be labeled with copper-64 at very low concentrations, with CBuDEDPA^{2-} providing the best radiolabeling efficiency. Furthermore, the radio-complexes of CHXDEDPA^{2-} and CBuDEDPA^{2-} show comparable stabilities in PBS and in the presence of excess DTPA as a competitor. This prompted us to develop a bifunctional analogue of CBuDEDPA^{2-}containing an NHBoc group at the cyclobutyl ring. However, while this structural modification had a minor impact in the radiolabeling efficiency, it is clearly detrimental in terms of radio-complex stability. We are currently developing alternative strategies toward bifunctional derivatives of this family of acyclic chelators, among which CHXDEDPA^{2-} displays the most promising properties in terms of thermodynamic stability and kinetic inertness, as judged by the DTPA competition experiments.

■ EXPERIMENTAL SECTION

General. Solvents and reagents were purchased from commercial sources and were directly used without further purification, unless otherwise stated. Anhydrous dichloromethane was freshly distilled when needed under a nitrogen atmosphere from calcium chloride. Anhydrous toluene was freshly distilled from sodium/benzophenone. TLC on silica gel-coated aluminum plates was performed in the systems indicated for each product in their description. The compounds were visualized by exposure to UV light at 254 nm, dipping in a basic potassium permanganate solution or in an acid vanillin solution. Flash chromatography purifications were carried out on silica gel (200−400 mesh) or on basic alumina (0.06−0.2 mm) using the solvent system specified for each product in the Supporting Information. Melting points were recorded on a Reicher Kofler block and values are uncorrected. IR spectra were obtained from samples in neat form with a BRUKER Alpha II spectrophotometer with an ATR (Attenuated Total Reflectance) accessory. Medium performance liquid chromatography was performed in a Puriflash XS 420 InterChim Chromatographer equipped with a UV-DAD detector in reverse phase, using a 20 g BGB Aquarius C18AQ reversed-phase column (100 Å, spherical, 15 μm). The experimental conditions are described below for each case. Preparative high performance liquid chromatography (HPLC) was performed using an Agilent 1260 Infinity II instrument equipped with an UV Variable Wavelenghth Detector, in manual injection and collection mode, using an Agilent InfinityLab ZORBAX 5 Eclipse Plus C18 (5 μm, 21.2 × 250 mm) and 10 mM ammonium acetate aqueous solution (phase A) and CH_3CN with 10% of phase A (phase B) as the mobile phases, operating at a flow rate of 20 mL/min. High-resolution electrospray-ionization time-of-flight (ESI-TOF) mass spectra were recorded in positive mode using a LTQ-Orbitrap Discovery Mass Spectrometer coupled to a Thermo Accela HPLC. Elemental analyses were obtained using a ThermoQuest Flash EA 1112 elemental analyzer. Aqueous solutions were lyophilized using a Biobase BK-FD10 Series apparatus. ^{1}H and ^{13}C NMR spectra of the ligands and their precursors were recorded on Bruker 300 MHz Ascend or Bruker 300 MHz AVANCE III, Bruker 400 MHz AVANCE III or Bruker AVANCE 500 spectrometers.

$^{64}CuCl_2$ was obtained from the University of Wisconsin Madison in a 0.1 M HCl solution. Radio-HPLC analysis was carried out using a Shimadzu HPLC-20AR chromatographer equipped with a binary gradient, pump, UV−vis detector, autoinjector, and Laura radio-detector on a Phenomenex Gemini C18 column (3 μm, 3 × 150 mm). Method A: (A) 0.1% TFA in water and (B) 0.1% TFA in CH_3CN with a flow rate of 0.8 mL min^{-1} (Gradient. 0−2 min: 5% B. 2−24 min: 5−95%B. 24−26 min: 95%B. 26−28 min: 95−5%B. 28−30 min: 5%B). Method B: (A) 10 mM NH_4OAc pH 7 (B) CH_3CN with a flow rate of 0.8 mL min^{-1} (Gradient. 0−2 min: 5% B. 2−24 min: 5−95%B. 24−28 min: 95% B. 28−30 min: 5% B) and UV detection at 220 and 254 nm. HPLC traces are shown in Figures S38−S39, Supporting Information.

Electrochemical Measurements. Cyclic voltammetry experiments were conducted using a three-electrode setup with an Autolab PGSTAT302 M potentiostat/galvanostat. The working electrode was a glassy carbon disk (Metrohm 61204600), which was polished with α-Al_2O_3 (0.3 μm) and rinsed with distilled water prior to each measurement. An Ag/AgCl reference electrode filled with 3 M KCl (Metrohm 6.0726.100) served as the reference electrode, while a platinum wire was used as the counter electrode. Prior to each measurement, the complex solutions containing 0.15 M NaCl were deoxygenated by bubbling nitrogen through them. Conditions:

https://doi.org/10.1021/acs.inorgchem.4c04050
Inorg. Chem. 2024, 63, 22297−22307

[Cu(CHXDEDPA)], 1.4 mM, pH 6.6; [Cu(CpDEDPA)], 1.3 mM, pH 6.9; [Cu(CBuDEDPA)], 1.3 mM, pH 5.0.

Thermodynamic Studies. Ligand protonation constants and stability constants of the complexes were determined using potentiometric and spectrophotometric titrations using HYPERQUAD.[67] All experimental data were collected at 25 °C using NaCl as inert electrolyte to keep constant the ionic strength (I = 1 M). Potentiometric titrations were conducted in a dual-wall thermostated cell with recirculating water to maintain a consistent temperature. To prevent CO_2 absorption, nitrogen was bubbled over the surface of the solution, and magnetic stirring was used to ensure thorough mixing. A Crison microBu 2030 automatic buret was employed to add the titrant, and the electromotive force (emf) was measured with a Crison micropH 2000 pH meter, which was connected to a Radiometer pHG211 glass electrode and a Radiometer REF201 reference electrode. Initially, 10 mL of a 1.5−2.0 mM chelator solution was added to the cell, and the pH was adjusted to 11 with NaOH. This solution was then titrated with a standard HCl solution to determine all protonation constant values within a single experiment. All potentiometric titrations were performed in duplicate. Due to the low pH at which dissociation occurs, the stability constants of all complexes were measured by spectrophotometry, as the glass electrode could not accurately determine these values. The electrode calibration was carried out using a standard method described in detail elsewhere.[68] Spectrophotometric titrations were performed with a Uvikon-XS (Bio-Tek Instruments) double-beam spectrophotometer, utilizing 1 cm path length quartz cuvettes and recording spectra in the range of 220 to 300 nm.

Dissociation Kinetics. Kinetic reducing reactions of the [Cu(CBuDEDPA)] complex were studied in phosphate buffer (∼0.2 M) of varying pH in the presence of ascorbate, which is able to reduce Cu(II) to Cu(I), and neocuproine, an efficient Cu(I) scavenger due to 1:2 complex formation ($[Cu(NC)_2]^+$). The reactions were monitored by conventional spectroscopy following the increase in absorbance at 450 nm due to the formation of the Cu(I)-neocuproine complex ($\varepsilon \approx 7000\ M^{-1}\cdot cm^{-1}$) and keeping the ratio [neocuproine]/[CuL] higher than ca. 2.5. Neocuproine was added upon dissolution in a small amount of dioxane (% v/v dioxane/water = 1.0−2% in the final solutions used for kinetics experiments). The ascorbate concentration (varying from 2 to 20 mM) was in high excess relative to complex concentration (∼10^{-4} M). All reactions were monitored by a Kontron-Uvikon 942 UV−vis spectrophotometer at 25 °C using 1 cm path length quartz cuvettes, with the complex being the last reagent added in the reaction mixture. In every case, absorbance (A) versus time (t) curves were appropriately fitted by a first-order integrated rate law [eq 2], with A_0, A_t, and A_∞ being the absorbance values at times zero, t, and at the end of the reaction, respectively, and k_0 being the calculated pseudo-first order rate constant.

$$A_t = A_\infty + (A_0 - A_\infty)\cdot e^{-k_0 t} \quad (2)$$

Ligand Stock Concentration. To determine the concentration of H_2CHXDEDPA, H_2CpDEDPA and H_2CBuDEDPA ligands used for radiolabeling experiments, spectrophotometric titrations were carried out with Cu^{2+}. The formation of [Cu(CHXDEDPA)], [Cu(CpDEDPA)] and [Cu(CBuDEDPA)] was monitored at 300 nm using a 1 cm path length cuvette and a NanoDrop spectrophotometer. The pH was adjusted to 5.5 using 10 mM ammonium acetate buffer. For H_2CHXDEDPA, a 1.78 mM ligand stock solution (60 μL) was titrated with addition of 10 μL (86.8 nmol) Cu^{2+} aliquots (as determined by ICP-OES) to determine the concentration of ligand by equivalents of Cu^{2+}. A 1.31 mM H_2CpDEDPA stock solution (80 μL) was titrated with addition of 10 μL (106.6 nmol) Cu^{2+} aliquots. For H_2CBuDEDPA, a 2.07 mM ligand stock solution (50 μL) was titrated with addition of 10 μL (146.9 nmol) Cu^{2+} aliquots. For H_2CBuDEDPA-NHBoc, a 1.41 mM (80 μL) ligand stock solution was titrated with addition of 10 μL (144.8 nmol) Cu^{2+} aliquots. The titration end point was determined when no further change in the absorbance intensity at 300 nm was added, testifying the complex formation (Figures S40−S43, Supporting Information).

^{64}Cu Radiolabeling. Two μL of the $^{64}CuCl_2$ stock solution was diluted in 0.05 M HCl to a total volume of 200 μL. The ligands were prepared from serial dilution of stock solutions (1, 0.25, 0.1, 0.025, 0.01, 0.0025, 0.001, 0.00025, 0.0001 mM) in deionized water. A 10 μL aliquot of each chelator stock solution (10, 2.5, 1.0, 0.25, 0.1, 0.025, 0.01, 0.0025, or 0.001 nmol, respectively) was diluted with 100 μL of ammonium acetate buffer (0.5 M, pH 5.5). A 50−90 μCi aliquot of $^{64}CuCl_2$ (6 μL) was then added and the solution was mixed thoroughly. The complexation was carried out at room temperature and the radiochemical yield was measured after 15, 30, and 60 min via radio-TLC on aluminum-backed silica plates with methanol as mobile phase. The degree of binding was quantified via autoradiography and integration of the signal of the bound complex (R_f = 0.5 for CHXDEDPA, R_f = 0.5 for CpDEDPA, 0.25 for CBuDEDPA and 0.48 for CBuDEDPA-NHBoc) vs the free ^{64}Cu (R_f = 0.04). The AMA was determined by ratio between the activity in the sample and the amount of ligand at 50% binding. All experiments were performed in triplicate.

Caution! Work with radioactive ^{64}Cu should only be carried out by trained personnel at facilities equipped to safely handle and store these radionuclides.

Stability in PBS. Experimental samples were prepared as previously described at a ligand concentration producing quantitative complex formation within 60 min (1 nmol). Once the labeling solution was prepared and quantitative formation of the desired ^{64}Cu complex was verified, a 15 μL aliquot of the labeling solution was added to 100 μL of 1× Dulbecco's phosphate-buffered saline. The stability of the complex was monitored by radio-TLC at 0, 1, 2, 3, 12, and 24 h.

DTPA Challenge. Radiolabeling stock solutions were prepared as previously described using 1 nmol of ligand. The radiolabeling solution was mixed with 100 μL of 10 mM DTPA solution. Transchelation was monitored by radio-TLC at 0, 1, 3, 12, and 24 h.

X-ray Diffraction Measurements. Single crystals of [Cu(CHXDEDPA)]·$(CH_3)_2CO\cdot H_2O$, [Cu(CpDEDPA)]·$4H_2O$ and [Cu(CBuDEDPA)] were analyzed by X-ray diffraction. Table S9 shows crystallographic data and the structure refinement parameters. Crystallographic data were collected at 100 K on a Bruker D8 Venture diffractometer with a Photon 100 CMOS detector and Mo Kα radiation (λ = 0.71073 Å) generated by an Incoatec high brillance microfocus source equipped with Incoatec Helios multilayer optics. The APEX3[69] software was used for collecting frames of data, indexing reflections, and the determination of lattice parameters, SAINT[70] for integration of intensity of reflections, and SADABS[71] for scaling and empirical absorption correction. The structures were solved by dual-space methods using the program SHELXT.[72] All non-hydrogen atoms were refined with anisotropic thermal parameters by full-matrix least-squares calculations on F^2 using the program SHELXL-2014.[72] For [Cu(CBuDEDPA)], the solvent mask command from Olex2 was used to correct the reflection data for the diffuse scattering due to the disordered molecules present in the unit cell. Hydrogen atoms of the compound were inserted at calculated positions and constrained with isotropic thermal parameters. Crystallographic data for the structures reported in this paper have been deposited with the Cambridge Crystallographic Data Centre as a supplementary publication no. 2382367−2382369, which can be obtained free of charge via www.ccdc.ac.uk/data_request/cif.

■ ASSOCIATED CONTENT

Supporting Information

The Supporting Information is available free of charge at https://pubs.acs.org/doi/10.1021/acs.inorgchem.4c04050.

Details on the synthesis and characterization of the chelators, additional spectroscopic, electrochemical, kinetic and HPLC data (PDF)

https://doi.org/10.1021/acs.inorgchem.4c04050
Inorg. Chem. 2024, 63, 22297−22307

Accession Codes

Deposition Numbers 2382367−2382369 contain the supplementary crystallographic data for this paper. These data can be obtained free of charge via the joint Cambridge Crystallographic Data Centre (CCDC) and Fachinformationszentrum Karlsruhe Access Structures service.

■ AUTHOR INFORMATION

Corresponding Authors

Eszter Boros − *Department of Chemistry, University of Wisconsin-Madison, Madison, Wisconsin 53706, United States;* orcid.org/0000-0002-4186-6586; Email: eboros@wisc.edu

Ona Illa − *Departament de Química, Universitat Autònoma de Barcelona, 08193 Cerdanyola del Vallès, Spain;* orcid.org/0000-0001-7390-4893; Email: ona.illa@uab.cat

Carlos Platas-Iglesias − *Centro Interdisciplinar de Química e Bioloxía (CICA) and Departamento de Química, Facultade de Ciencias, Universidade da Coruña, 15071 A Coruña, Spain;* orcid.org/0000-0002-6989-9654; Email: carlos.platas.iglesias@udc.es

Authors

Daniel Torralba-Maldonado − *Departament de Química, Universitat Autònoma de Barcelona, 08193 Cerdanyola del Vallès, Spain*

Axia Marlin − *Department of Chemistry, University of Wisconsin-Madison, Madison, Wisconsin 53706, United States*

Fátima Lucio-Martínez − *Centro Interdisciplinar de Química e Bioloxía (CICA) and Departamento de Química, Facultade de Ciencias, Universidade da Coruña, 15071 A Coruña, Spain;* orcid.org/0000-0002-4505-2360

Antía Freire-García − *Centro Interdisciplinar de Química e Bioloxía (CICA) and Departamento de Química, Facultade de Ciencias, Universidade da Coruña, 15071 A Coruña, Spain;* orcid.org/0000-0002-5974-4464

Jennifer Whetter − *Department of Chemistry, University of Wisconsin-Madison, Madison, Wisconsin 53706, United States*

Isabel Brandariz − *Centro Interdisciplinar de Química e Bioloxía (CICA) and Departamento de Química, Facultade de Ciencias, Universidade da Coruña, 15071 A Coruña, Spain*

Emilia Iglesias − *Centro Interdisciplinar de Química e Bioloxía (CICA) and Departamento de Química, Facultade de Ciencias, Universidade da Coruña, 15071 A Coruña, Spain*

Paulo Pérez-Lourido − *Departamento de Química Inorgánica, Facultad de Química, Universidade de Vigo, 36310 Pontevedra, Spain;* orcid.org/0000-0003-2281-3064

Rosa M. Ortuño − *Departament de Química, Universitat Autònoma de Barcelona, 08193 Cerdanyola del Vallès, Spain;* orcid.org/0000-0001-7635-7354

David Esteban-Gómez − *Centro Interdisciplinar de Química e Bioloxía (CICA) and Departamento de Química, Facultade de Ciencias, Universidade da Coruña, 15071 A Coruña, Spain;* orcid.org/0000-0001-6270-1660

Complete contact information is available at: https://pubs.acs.org/10.1021/acs.inorgchem.4c04050

Notes

The authors declare no competing financial interest.

■ ACKNOWLEDGMENTS

Authors thank Ministerio de Ciencia e Innovación (Grants PID2022-138335NB-I00, PID2022-139826OB-I00 and RED2022-134091-T) and Xunta de Galicia (ED431C 2023/33) for generous financial support. D.T.-M. thanks the Generalitat de Catalunya (Grant 2020 FI-SDUR-00055) and A. F.-G. thanks Ministerio de Universidades (Grant FPU21/06305) for funding their Ph.D. contract. P.P.-L. is indebted to CACTI (Universidade de Vigo) for X-ray measurements.

■ REFERENCES

(1) Chakravarty, R.; Chakraborty, S.; Dash, A. $^{64}Cu^{2+}$ Ions as PET Probe: An Emerging Paradigm in Molecular Imaging of Cancer. *Mol. Pharmaceutics* **2016**, *13* (11), 3601−3612.

(2) Smith, S. V. Molecular Imaging with Copper-64. *J. Inorg. Biochem.* **2004**, *98* (11), 1874−1901.

(3) Jha, A.; Patel, M.; Carrasquillo, J. A.; Chen, C. C.; Millo, C.; Maass-Moreno, R.; Ling, A.; Lin, F. I.; Lechan, R. M.; Hope, T. A.; Taïeb, D.; Civelek, A. C.; Pacak, K. Choice Is Good at Times: The Emergence of [^{64}Cu]Cu-DOTATATE−Based Somatostatin Receptor Imaging in the Era of [^{68}Ga]Ga-DOTATATE. *J. Nucl. Med.* **2022**, *63* (9), 1300−1301.

(4) Zhang, Y.; Hong, H.; Engle, J. W.; Bean, J.; Yang, Y.; Leigh, B. R.; Barnhart, T. E.; Cai, W. Positron Emission Tomography Imaging of CD105 Expression with a ^{64}Cu-Labeled Monoclonal Antibody: NOTA Is Superior to DOTA. *PLoS One* **2011**, *6* (12), No. e28005.

(5) De Silva, R. A.; Jain, S.; Lears, K. A.; Chong, H.-S.; Kang, C. S.; Sun, X.; Rogers, B. E. Copper-64 Radiolabeling and Biological Evaluation of Bifunctional Chelators for Radiopharmaceutical Development. *Nucl. Med. Biol.* **2012**, *39* (8), 1099−1104.

(6) Maheshwari, V.; Dearling, J. L. J.; Treves, S. T.; Packard, A. B. Measurement of the Rate of Copper(II) Exchange for 64Cu Complexes of Bifunctional Chelators. *Inorg. Chim. Acta* **2012**, *393*, 318−323.

(7) Cooper, M. S.; Ma, M. T.; Sunassee, K.; Shaw, K. P.; Williams, J. D.; Paul, R. L.; Donnelly, P. S.; Blower, P. J. Comparison of ^{64}Cu-Complexing Bifunctional Chelators for Radioimmunoconjugation: Labeling Efficiency, Specific Activity, and *in Vitro/in Vivo* Stability. *Bioconjugate Chem.* **2012**, *23* (5), 1029−1039.

(8) Vahidfar, N.; Bakhshi Kashi, M.; Afshar, S.; Sheikhzadeh, P.; Farzanefar, S.; Salehi, Y.; Delpasand, E.; N Molloy, E.; Mirzaei, S.; Ahmadzadehfar, H.; Eppard, E. Recent Advances of Copper-64 Based Radiopharmaceuticals in Nuclear Medicine. In *Advances in Dosimetry and New Trends in Radiopharmaceuticals*; Adelaja Osibote, O., Eppard, E., Eds.; IntechOpen, 2024; ..

(9) Brody, S. L.; Gunsten, S. P.; Luehmann, H. P.; Sultan, D. H.; Hoelscher, M.; Heo, G. S.; Pan, J.; Koenitzer, J. R.; Lee, E. C.; Huang, T.; Mpoy, C.; Guo, S.; Laforest, R.; Salter, A.; Russell, T. D.; Shifren, A.; Combadiere, C.; Lavine, K. J.; Kreisel, D.; Humphreys, B. D.; Rogers, B. E.; Gierada, D. S.; Byers, D. E.; Gropler, R. J.; Chen, D. L.; Atkinson, J. J.; Liu, Y. Chemokine Receptor 2−Targeted Molecular Imaging in Pulmonary Fibrosis. A Clinical Trial. *Am. J. Respir. Crit. Care Med.* **2021**, *203* (1), 78−89.

(10) Izquierdo-Garcia, D.; Désogère, P.; Philip, A. L.; Mekkaoui, C.; Weiner, R. B.; Catalano, O. A.; Iris Chen, Y.-C.; DeFaria Yeh, D.; Mansour, M.; Catana, C.; Caravan, P.; Sosnovik, D. E. Detection and Characterization of Thrombosis in Humans Using Fibrin-Targeted Positron Emission Tomography and Magnetic Resonance. *JACC Cardiovasc. Imaging* **2022**, *15* (3), 504.

(11) Laforest, R.; Ghai, A.; Fraum, T. J.; Oyama, R.; Frye, J.; Kaemmerer, H.; Gaehle, G.; Voller, T.; Mpoy, C.; Rogers, B. E.; Fiala, M.; Shoghi, K. I.; Achilefu, S.; Rettig, M.; Vij, R.; DiPersio, J. F.; Schwarz, S.; Shokeen, M.; Dehdashti, F. First-in-Humans Evaluation

of Safety and Dosimetry of ^{64} Cu-LLP2A for PET Imaging. *J. Nucl. Med.* **2023**, *64* (2), 320−328.

(12) McInnes, L. E.; Cullinane, C.; Roselt, P. D.; Jackson, S.; Blyth, B. J.; Van Dam, E. M.; Zia, N. A.; Harris, M. J.; Hicks, R. J.; Donnelly, P. S. Therapeutic Efficacy of a Bivalent Inhibitor of Prostate-Specific Membrane Antigen Labeled with ^{67} Cu. *J. Nucl. Med.* **2021**, *62* (6), 829−832.

(13) Hicks, R. J.; Jackson, P.; Kong, G.; Ware, R. E.; Hofman, M. S.; Pattison, D. A.; Akhurst, T. A.; Drummond, E.; Roselt, P.; Callahan, J.; Price, R.; Jeffery, C. M.; Hong, E.; Noonan, W.; Herschtal, A.; Hicks, L. J.; Hedt, A.; Harris, M.; Paterson, B. M.; Donnelly, P. S. ^{64} Cu-SARTATE PET Imaging of Patients with Neuroendocrine Tumors Demonstrates High Tumor Uptake and Retention, Potentially Allowing Prospective Dosimetry for Peptide Receptor Radionuclide Therapy. *J. Nucl. Med.* **2019**, *60* (6), 777−785.

(14) Comba, P.; Kubeil, M.; Pietzsch, J.; Rudolf, H.; Stephan, H.; Zarschler, K. Bispidine Dioxotetraaza Macrocycles: A New Class of Bispidines for ^{64}Cu PET Imaging. *Inorg. Chem.* **2014**, *53* (13), 6698−6707.

(15) Knighton, R. C.; Troadec, T.; Mazan, V.; Le Saëc, P.; Marionneau-Lambot, S.; Le Bihan, T.; Saffon-Merceron, N.; Le Bris, N.; Chérel, M.; Faivre-Chauvet, A.; Elhabiri, M.; Charbonnière, L. J.; Tripier, R. Cyclam-Based Chelators Bearing Phosphonated Pyridine Pendants for ^{64}Cu-PET Imaging: Synthesis, Physicochemical Studies, Radiolabeling, and Bioimaging. *Inorg. Chem.* **2021**, *60* (4), 2634−2648.

(16) Bandara, N.; Sharma, A. K.; Krieger, S.; Schultz, J. W.; Han, B. H.; Rogers, B. E.; Mirica, L. M. Evaluation of ^{64}Cu-Based Radiopharmaceuticals that Target Aβ Peptide Aggregates as Diagnostic Tools for Alzheimer's Disease. *J. Am. Chem. Soc.* **2017**, *139* (36), 12550−12558.

(17) Cho, H.-J.; Huynh, T. T.; Rogers, B. E.; Mirica, L. M. Design of a Multivalent Bifunctional Chelator for Diagnostic ^{64} Cu PET Imaging in Alzheimer's Disease. *Proc. Natl. Acad. Sci. U.S.A.* **2020**, *117* (49), 30928−30933.

(18) Brown, A. M.; Butman, J. L.; Lengacher, R.; Vargo, N. P.; Martin, K. E.; Koller, A.; Śmiłowicz, D.; Boros, E.; Robinson, J. R. N. *N,N*-Alkylation Clarifies the Role of *N*- and *O*-Protonated Intermediates in Cyclen-Based ^{64}Cu Radiopharmaceuticals. *Inorg. Chem.* **2023**, *62* (4), 1362−1376.

(19) Martin, S.; Maus, S.; Stemler, T.; Rosar, F.; Khreish, F.; Holland, J. P.; Ezziddin, S.; Bartholomä, M. D. Proof-of-Concept Study of the NOTI Chelating Platform: Preclinical Evaluation of 64Cu-Labeled Mono- and Trimeric c(RGDfK) Conjugates. *Mol. Imaging Biol.* **2021**, *23* (1), 95−108.

(20) Guillou, A.; Lima, L. M. P.; Esteban-Gómez, D.; Le Poul, N.; Bartholomä, M. D.; Platas-Iglesias, C.; Delgado, R.; Patinec, V.; Tripier, R. Methylthiazolyl Tacn Ligands for Copper Complexation and Their Bifunctional Chelating Agent Derivatives for Bioconjugation and Copper-64 Radiolabeling: An Example with Bombesin. *Inorg. Chem.* **2019**, *58* (4), 2669−2685.

(21) Roux, A.; Gillet, R.; Huclier-Markai, S.; Ehret-Sabatier, L.; Charbonnière, L. J.; Nonat, A. M. Bifunctional Bispidine Derivatives for Copper-64 Labelling and Positron Emission Tomography. *Org. Biomol. Chem.* **2017**, *15* (6), 1475−1483.

(22) Kubeil, M.; Neuber, C.; Starke, M.; Arndt, C.; Rodrigues Loureiro, L.; Hoffmann, L.; Feldmann, A.; Bachmann, M.; Pietzsch, J.; Comba, P.; Stephan, H. 64Cu Tumor Labeling with Hexadentate Picolinic Acid-Based Bispidine Immunoconjugates. *Chem.—Eur. J.* **2024**, *30* (32), No. e202400366.

(23) David, T.; Hlinová, V.; Kubíček, V.; Bergmann, R.; Striese, F.; Berndt, N.; Szöllősi, D.; Kovács, T.; Máthé, D.; Bachmann, M.; Pietzsch, H.-J.; Hermann, P. Improved Conjugation, 64-Cu Radiolabeling, in Vivo Stability, and Imaging Using Nonprotected Bifunctional Macrocyclic Ligands: Bis(Phosphinate) Cyclam (BPC) Chelators. *J. Med. Chem.* **2018**, *61* (19), 8774−8796.

(24) Guo, Y.; Ferdani, R.; Anderson, C. J. Preparation and Biological Evaluation of ^{64}Cu Labeled Tyr ^{3} -Octreotate Using a Phosphonic Acid-Based Cross-Bridged Macrocyclic Chelator. *Bioconjugate Chem.* **2012**, *23* (7), 1470−1477.

(25) Ferreirós-Martínez, R.; Esteban-Gómez, D.; Platas-Iglesias, C.; De Blas, A.; Rodríguez-Blas, T. Zn(II), Cd(II) and Pb(II) Complexation with Pyridinecarboxylate Containing Ligands. *Dalton Trans.* **2008**, No. 42, 5754.

(26) Boros, E.; Ferreira, C. L.; Cawthray, J. F.; Price, E. W.; Patrick, B. O.; Wester, D. W.; Adam, M. J.; Orvig, C. Acyclic Chelate with Ideal Properties for ^{68}Ga PET Imaging Agent Elaboration. *J. Am. Chem. Soc.* **2010**, *132* (44), 15726−15733.

(27) Ramogida, C. F.; Cawthray, J. F.; Boros, E.; Ferreira, C. L.; Patrick, B. O.; Adam, M. J.; Orvig, C. H_2*CHX*Dedpa and H_4*CHX*Octapa—Chiral Acyclic Chelating Ligands for $^{67/68}$Ga and ^{111}In Radiopharmaceuticals. *Inorg. Chem.* **2015**, *54* (4), 2017−2031.

(28) Boros, E.; Cawthray, J. F.; Ferreira, C. L.; Patrick, B. O.; Adam, M. J.; Orvig, C. Evaluation of the H_2**Dedpa** Scaffold and Its cRGDyK Conjugates for Labeling with ^{64}Cu. *Inorg. Chem.* **2012**, *51* (11), 6279−6284.

(29) Ramogida, C. F.; Boros, E.; Patrick, B. O.; Zeisler, S. K.; Kumlin, J.; Adam, M. J.; Schaffer, P.; Orvig, C. Evaluation of H_2CHXdedpa, H_2Dedpa- and H_2CHXdedpa-N,N′-Propyl-2-NI Ligands for ^{64}Cu(ii) Radiopharmaceuticals. *Dalton Trans.* **2016**, *45* (33), 13082−13090.

(30) Ramogida, C. F.; Murphy, L.; Cawthray, J. F.; Ross, J. D.; Adam, M. J.; Orvig, C. Novel "Bi-Modal" H_2Dedpa Derivatives for Radio- and Fluorescence Imaging. *J. Inorg. Biochem.* **2016**, *162*, 253−262.

(31) Ramogida, C. F.; Pan, J.; Ferreira, C. L.; Patrick, B. O.; Rebullar, K.; Yapp, D. T. T.; Lin, K.-S.; Adam, M. J.; Orvig, C. Nitroimidazole-Containing H_2Dedpa and H_2*CHX*Dedpa Derivatives as Potential PET Imaging Agents of Hypoxia with ^{68}Ga. *Inorg. Chem.* **2015**, *54* (10), 4953−4965.

(32) Pena-Bonhome, C.; Fiaccabrino, D.; Rama, T.; Fernández-Pavón, D.; Southcott, L.; Zhang, Z.; Lin, K.-S.; De Blas, A.; Patrick, B. O.; Schaffer, P.; Orvig, C.; Jaraquemada-Peláez, M. d. G.; Rodríguez-Blas, T. Toward ^{68}Ga and ^{64}Cu Positron Emission Tomography Probes: Is H_2Dedpa-*N,N*′-Pram the Missing Link for Dedpa Conjugation? *Inorg. Chem.* **2023**, *62* (50), 20593−20607.

(33) Bailey, G. A.; Price, E. W.; Zeglis, B. M.; Ferreira, C. L.; Boros, E.; Lacasse, M. J.; Patrick, B. O.; Lewis, J. S.; Adam, M. J.; Orvig, C. H_2Azapa: A Versatile Acyclic Multifunctional Chelator for ^{67}Ga, ^{64}Cu, ^{111}In, and ^{177}Lu. *Inorg. Chem.* **2012**, *51* (22), 12575−12589.

(34) Caneda-Martínez, L.; Valencia, L.; Fernández-Pérez, I.; Regueiro-Figueroa, M.; Angelovski, G.; Brandariz, I.; Esteban-Gómez, D.; Platas-Iglesias, C. Toward Inert Paramagnetic Ni(ii)-Based Chemical Exchange Saturation Transfer MRI Agents. *Dalton Trans.* **2017**, *46* (43), 15095−15106.

(35) Uzal-Varela, R.; Lucio-Martínez, F.; Nucera, A.; Botta, M.; Esteban-Gómez, D.; Valencia, L.; Rodríguez-Rodríguez, A.; Platas-Iglesias, C. A Systematic Investigation of the NMR Relaxation Properties of Fe(iii)-EDTA Derivatives and Their Potential as MRI Contrast Agents. *Inorg. Chem. Front.* **2023**, *10* (5), 1633−1649.

(36) Porcar-Tost, O.; Olivares, J. A.; Pallier, A.; Esteban-Gómez, D.; Illa, O.; Platas-Iglesias, C.; Tóth, É.; Ortuño, R. M. Gadolinium Complexes of Highly Rigid, Open-Chain Ligands Containing a Cyclobutane Ring in the Backbone: Decreasing Ligand Denticity Might Enhance Kinetic Inertness. *Inorg. Chem.* **2019**, *58* (19), 13170−13183.

(37) Porcar-Tost, O.; Pallier, A.; Esteban-Gómez, D.; Illa, O.; Platas-Iglesias, C.; Tóth, É.; Ortuño, R. M. Stability, Relaxometric and Computational Studies on Mn^{2+} Complexes with Ligands Containing a Cyclobutane Scaffold. *Dalton Trans.* **2021**, *50* (3), 1076−1085.

(38) Platas-Iglesias, C.; Mato-Iglesias, M.; Djanashvili, K.; Muller, R. N.; Elst, L. V.; Peters, J. A.; de Blas, A.; Rodríguez-Blas, T. Lanthanide Chelates Containing Pyridine Units with Potential Application as Contrast Agents in Magnetic Resonance Imaging. *Chem.—Eur. J.* **2004**, *10* (14), 3579−3590.

(39) Chang, Z.; Boyaud, F.; Guillot, R.; Boddaert, T.; Aitken, D. J. A Photochemical Route to 3- and 4-Hydroxy Derivatives of 2-

Aminocyclobutane-1-Carboxylic Acid with an All-Cis Geometry. *J. Org. Chem.* **2018**, *83* (1), 527−534.
(40) Kálmán, F. K.; Végh, A.; Regueiro-Figueroa, M.; Tóth, É.; Platas-Iglesias, C.; Tircsó, G. H_4Octapa: Highly Stable Complexation of Lanthanide(III) Ions and Copper(II). *Inorg. Chem.* **2015**, *54* (5), 2345−2356.
(41) Ammeter, J.; Buergi, H. B.; Gamp, E.; Meyer-Sandrin, V.; Jensen, W. P. Static and Dynamic Jahn-Teller Distortions in CuN6 Complexes. Crystal Structures and EPR Spectra of Complexes between Copper(II) and Rigid, Tridentate Cis,Cis-1,3,5-Triaminocyclohexane (Tach: Cu(Tach)2(ClO4)2, Cu(Tach)2(NO3)2. Crystal Structure of Ni(Tach)2(NO3)2. *Inorg. Chem.* **1979**, *18* (3), 733−750.
(42) Deeth, R. J.; Hitchman, M. A. Factors Influencing Jahn-Teller Distortions in Six-Coordinate Copper(II) and Low-Spin Nickel(II) Complexes. *Inorg. Chem.* **1986**, *25* (8), 1225−1233.
(43) Alvarez, S.; Avnir, D.; Llunell, M.; Pinsky, M. Continuous symmetry maps and shape classification. The case of six-coordinated metal compoundsElectronic supplementary information (ESI) available: tables of CSD refcodes, structural parameters and symmetry measures for the studied compounds. See http://www.rsc.org/suppdata/nj/b2/b202096n/. *New J. Chem.* **2002**, *26* (8), 996−1009.
(44) Alvarez, S. Polyhedra in (Inorganic) Chemistry. *Dalton Trans.* **2005**, *13*, 2209.
(45) Pinsky, M.; Avnir, D. Continuous Symmetry Measures. 5. The Classical Polyhedra. *Inorg. Chem.* **1998**, *37* (21), 5575−5582.
(46) Casanova, D.; Cirera, J.; Llunell, M.; Alemany, P.; Avnir, D.; Alvarez, S. Minimal Distortion Pathways in Polyhedral Rearrangements. *J. Am. Chem. Soc.* **2004**, *126* (6), 1755−1763.
(47) Uzal-Varela, R.; Patinec, V.; Tripier, R.; Valencia, L.; Maneiro, M.; Canle, M.; Platas-Iglesias, C.; Esteban-Gómez, D.; Iglesias, E. On the Dissociation Pathways of Copper Complexes Relevant as PET Imaging Agents. *J. Inorg. Biochem.* **2022**, *236*, 111951.
(48) Wadas, T. J.; Wong, E. H.; Weisman, G. R.; Anderson, C. J. Coordinating Radiometals of Copper, Gallium, Indium, Yttrium, and Zirconium for PET and SPECT Imaging of Disease. *Chem. Rev.* **2010**, *110* (5), 2858−2902.
(49) Elgrishi, N.; Rountree, K. J.; McCarthy, B. D.; Rountree, E. S.; Eisenhart, T. T.; Dempsey, J. L. A Practical Beginner's Guide to Cyclic Voltammetry. *J. Chem. Educ.* **2018**, *95* (2), 197−206.
(50) Salinas, G.; Ibanez, J. G.; Vásquez-Medrano, R.; Frontana-Uribe, B. A. Analysis of Cu in Mezcal Commercial Samples Using Square Wave Anodic Stripping Voltammetry. *J. Electrochem. Sci. Technol.* **2018**, *9* (4), 276−281.
(51) Friis, E. P.; Andersen, J. E. T.; Madsen, L. L.; Bonander, N.; Møller, P.; Ulstrup, J. Dynamics of Pseudomonas Aeruginosa Azurin and Its Cys3Ser. Mutant at Single-Crystal Gold Surfaces Investigated by Cyclic Voltammetry and Atomic Force Microscopy. **1998**, *43*, 1114−1122, .
(52) Banks, C. V.; Bystroff, R. I. Stability Orders in Transition Metal-1,10-Phenanthroline Complexes [1]. *J. Am. Chem. Soc.* **1959**, *81* (23), 6153−6158.
(53) Irving, H.; Williams, R. J. P. 637. The stability of transition-metal complexes. *J. Chem. Soc.* **1953**, 3192−3210.
(54) Kálmán, F. K.; Tircsó, G. Kinetic Inertness of the Mn^{2+} Complexes Formed with AAZTA and Some Open-Chain EDTA Derivatives. *Inorg. Chem.* **2012**, *51* (19), 10065−10067.
(55) Zhang, T.; Liu, J.-M.; Huang, X.-F.; Xia, B.; Su, C.-Y.; Luo, G.-F.; Xu, Y.-W.; Wu, Y.-X.; Mao, Z.-W.; Qiu, R.-L. Chelant Extraction of Heavy Metals from Contaminated Soils Using New Selective EDTA Derivatives. *J. Hazard. Mater.* **2013**, *262*, 464−471.
(56) Vágner, A.; D'Alessandria, C.; Gambino, G.; Schwaiger, M.; Aime, S.; Maiocchi, A.; Tóth, I.; Baranyai, Z.; Tei, L. A Rigidified AAZTA-like Ligand as Efficient Chelator for ^{68}Ga Radiopharmaceuticals. *ChemistrySelect* **2016**, *1* (2), 163−171.
(57) Harris, W. R.; Raymond, K. N.; Weitl, F. L. Ferric Ion Sequestering Agents. 6. The Spectrophotometric and Potentiometric Evaluation of Sulfonated Tricatecholate Ligands. *J. Am. Chem. Soc.* **1981**, *103* (10), 2667−2675.
(58) Tircsó, G.; Tircsóné Benyó, E.; Garda, Z.; Singh, J.; Trokowski, R.; Brücher, E.; Sherry, A. D.; Tóth, E.-.; Kovács, Z. Comparison of the Equilibrium, Kinetic and Water Exchange Properties of Some Metal Ion-DOTA and DOTA-Bis(Amide) Complexes. *J. Inorg. Biochem.* **2020**, *206*, 111042.
(59) Bevilacqua, A.; Gelb, R. I.; Hebard, W. B.; Zompa, L. J. Equilibrium and Thermodynamic Study of the Aqueous Complexation of 1,4,7-Triazacyclononane-N,N',N''-Triacetic Acid with Protons, Alkaline-Earth-Metal Cations, and Copper(II). *Inorg. Chem.* **1987**, *26* (16), 2699−2706.
(60) Kubíček, V.; Böhmová, Z.; Ševčíková, R.; Vaněk, J.; Lubal, P.; Poláková, Z.; Michalicová, R.; Kotek, J.; Hermann, P. NOTA Complexes with Copper(II) and Divalent Metal Ions: Kinetic and Thermodynamic Studies. *Inorg. Chem.* **2018**, *57* (6), 3061−3072.
(61) Comba, P.; Grimm, L.; Orvig, C.; Rück, K.; Wadepohl, H. Synthesis and Coordination Chemistry of Hexadentate Picolinic Acid Based Bispidine Ligands. *Inorg. Chem.* **2016**, *55* (24), 12531−12543.
(62) Sun, X.; Wuest, M.; Weisman, G. R.; Wong, E. H.; Reed, D. P.; Boswell, C. A.; Motekaitis, R.; Martell, A. E.; Welch, M. J.; Anderson, C. J. Radiolabeling and In Vivo Behavior of Copper-64-Labeled Cross-Bridged Cyclam Ligands. *J. Med. Chem.* **2002**, *45* (2), 469−477.
(63) Voráčová, I.; Vaněk, J.; Pasulka, J.; Střelcová, Z.; Lubal, P.; Hermann, P. Dissociation Kinetics Study of Copper(II) Complexes of DO3A, DOTA and Its Monosubstituted Derivatives. *Polyhedron* **2013**, *61*, 99−104.
(64) Ševčík, R.; Vaněk, J.; Michalicová, R.; Lubal, P.; Hermann, P.; Santos, I. C.; Santos, I.; Campello, M. P. C. Formation and Decomplexation Kinetics of Copper(ii) Complexes with Cyclen Derivatives Having Mixed Carboxylate and Phosphonate Pendant Arms. *Dalton Trans.* **2016**, *45* (32), 12723−12733.
(65) Kotek, J.; Lubal, P.; Hermann, P.; Císařová, I.; Lukeš, I.; Godula, T.; Svobodová, I.; Táborský, P.; Havel, J. High Thermodynamic Stability and Extraordinary Kinetic Inertness of Copper(II) Complexes with 1,4,8,11-Tetraazacyclotetradecane-1,8-Bis-(Methylphosphonic Acid): Example of a Rare Isomerism between Kinetically Inert Penta- and Hexacoordinated Copper(II) Complexes. *Chem.—Eur. J.* **2003**, *9* (1), 233−248.
(66) Gahler, A. R. Colorimetric Determination of Copper with Neo-Cuproine. *Anal. Chem.* **1954**, *26* (3), 577−579.
(67) Gans, P.; Sabatini, A.; Vacca, A. Investigation of Equilibria in Solution. Determination of Equilibrium Constants with the HYPERQUAD Suite of Programs. *Talanta* **1996**, *43* (10), 1739−1753.
(68) Harriswangler, C.; McNeil, B. L.; Brandariz-Lendoiro, I.; Lucio-Martínez, F.; Valencia, L.; Esteban-Gómez, D.; Ramogida, C. F.; Platas-Iglesias, C. Exploring the Use of Rigid 18-Membered Macrocycles with Amide Pendant Arms for Pb(ii)-Based Radiopharmaceuticals. *Inorg. Chem. Front.* **2024**, *11* (4), 1070−1086.
(69) APEX3, 2016..
(70) *SAINT Version 8.37A*; Bruker AXS Inc.; Madison, Wisconsin, USA, 2015..
(71) Sheldrick, G. M. *SADABS*, 2014.
(72) Sheldrick, G. M. Crystal Structure Refinement with *SHELXL*, Version 2014/5. *Acta Crystallogr. Sect. C Struct. Chem.* **2015**, *71* (1), 3−8.

https://doi.org/10.1021/acs.inorgchem.4c04050
Inorg. Chem. 2024, 63, 22297−22307